# The Complexity of Measuring and Representing the Hygroscopicity of Mixed Component Aerosol

Aleksandra Marsh,[1] Grazia Rovelli,[1] Rachael E. H. Miles[1] and Jonathan P. Reid[1,*]

[1]School of Chemistry, University of Bristol, Cantock's Close, Bristol, BS8 1TS, UK

* *Correspondence to*: Jonathan P. Reid (J.P.Reid@bristol.ac.uk)

**Abstract**

The validation of approaches to predict the hygroscopicity of complex mixtures of organic components in aerosol is important for understanding the hygroscopic response of organic aerosol in the atmosphere. We report new measurements of the hygroscopicity of mixtures of dicarboxylic acids and amino acids using a comparative kinetic electrodynamic balance (CK-EDB) approach, inferring the equilibrium water content of the aerosol from close to a saturation relative humidity (100 %) down to 80 %. We show that the solution densities and refractive indices of the mixtures can be estimated with an accuracy of better than ±2 % using the molar refractive index mixing rule and densities and refractive indices for the individual binary organic-aqueous solutions. Further, we show that the often-used mass, volume and mole-weighted mixing rules to estimate the hygroscopicity parameter κ can over-estimate the hygroscopic parameter by a factor of as much as 3, highlighting the need to understand the specific non-ideal interactions that may arise synergistically in mixtures and cannot be represented by simple models. Indeed, in some extreme cases the hygroscopicity of a multicomponent mixture can be very close to that for the least hygroscopic component. For mixtures of similar components for which no additional synergistic interactions need be considered, the hygroscopicity of the mixed component aerosol can be estimated with high accuracy from the hygroscopic response of the binary aqueous-organic aerosol. In conclusion, we suggest that the hygroscopicity of multicomponent organic aerosol can be highly non-additive and that simple correlations of hygroscopicity with composition may often misrepresent the level of complexity essential to interpret aerosol hygroscopicity.

## 1. Introduction

The extent of water uptake by ambient aerosol is critical to understanding the size distribution of aerosol particles and, consequently, the radiative balance of the Earth and the impact of aerosols on human health. The hygroscopic response of aerosol particles (the ability of a particle to absorb water) impacts climate directly via scattering and absorption of incoming solar radiation and indirectly by affecting cloud formation processes (i.e. cloud condensation nuclei activity) and lifetimes.[1, 2] Hygroscopic growth can also lead to the co-condensation of semi-volatile organic compounds leading to an increase in the partitioning of organic mass to the condensed aerosol phase.[3] Upon inhalation, the penetration of ambient aerosol into the respiratory system is influenced by the aerosol hygroscopicity, with the potential to affect associated morbidity and mortality rates.[4-7] In addition, the physicochemical properties of aerosol particles (e.g. viscosity, surface tension, optical properties) depend on the liquid water content.[8, 9]

Ambient aerosols are complex in composition, containing a myriad of organic and inorganic species and continuously evolving in chemical composition through reactions, such as oxidation, oligomerisation and photochemistry,[10, 11] and gas-particle partitioning. Fine aerosol mass (particle diameters <1 μm) is dominated by organic species with variable physical and chemical properties [12] covering a broad spectrum in molecular weight, level of oxidation and solubility. Understanding the behaviour of organic aerosol and quantifying their impacts on climate and human health is challenging because of the complex and evolving chemical composition. Laboratory-based hygroscopicity measurements have focused on using proxies of ambient aerosol (e.g. sodium chloride, dicarboxylic acids [13] and saccharides to mimic marine, organic or SOA respectively) or on measurements of laboratory generated SOA obtained from the chemical evolution of oxidised gaseous precursors in a smog chamber.[14]

Petters and Kreidenweis introduced the hygroscopicity parameter kappa (κ) to represent the hygroscopic properties of a solute using a single value; κ was primarily introduced to allow aerosol hygroscopic properties to be easily included in global climate modelling.[15] Frequently, values of κ are correlated with the O:C ratio of laboratory or field samples of unknown chemical composition [16, 17] in an attempt to establish simple relationships between the overall composition of complex aerosol systems and their hygroscopic properties. In laboratory experiments on multicomponent mixtures, the mass, mole and volume weightings of the single components κ can be used to determine the hygroscopicity of a mixture of solutes. However, the applicability of these mixing rules relies on the assumption of additive hygroscopic behaviour.[15]

There are few systematic studies of the additivity of hygroscopic response for multicomponent mixtures of organic solutes with increasing mixture complexity. In fact, the available literature on the hygroscopicity of compositionally complex mixtures focuses on organic and inorganic mixtures and, in most examples, a Hygroscopicity Tandem Differential Mobility Analyser (HTDMA) is used in the retrieval of the hygroscopic response.[18-25] Sodium chloride or ammonium sulphate is often used as the inorganic component. Although soluble inorganic components may often contribute little to the total aerosol mass, they can play a significant

role in determining the activity of cloud condensation nuclei (see for example Roberts et al.),[26] a clear indicator of the often non-additive nature of aerosol hygroscopic response. A number of authors have considered the hygroscopicity of mixed component aerosols containing mixtures of dicarboxylic acids[27, 28] and mixtures of dicarboxylic acids with inorganic salts.[29] Lui et al. determined the hygroscopicity of phthalic acid or levoglucosan combined with ammonium sulphate or ammonium nitrate using a HTDMA, with results in good agreement with predictions from E-AIM.[20] Mikhailov and co-workers applied a mass-based hygroscopicity parameter interaction model to interpret experimental measurements obtained using a HTDMA.[24] First, single component aqueous solutions were considered; then the mass based hygroscopicity parameter was applied to mixtures of ammonium sulphate and malonic acid. Marcolli and co-workers reported the water uptake properties and the deliquescence RH of droplets containing a five-component organic mixture containing malic, malonic, maleic, glutaric, and methyl-succinic acids using a HTDMA.[25] They observed that the deliquescence RH was lowered for progressively complex mixtures and was further lowered upon the addition of sodium chloride to the organic mixture.

In all the examples discussed above, measurements were made for accumulation mode particle sizes using an HTDMA. Measurements at high RHs using these approaches can be challenging, particularly at an RH above 90%. Work by Suda and Petters introduced the use of ammonium sulphate aerosol as a probe system to determine the gas phase RH prior to a scan of a sample of unknown hygroscopicity.[30] Whilst this affords improvement in RH determination, the time required for the probe aerosol scans and the frequency of these scans (approximately every 20 minutes) may not be able to account for fluctuations in the RH on shorter timescales.[30] By contrast, the electrodynamic balance (EDB) and the comparative kinetics (CK) approach used in this work, validated in previous studies,[31-33] allows very accurate determination of the RH experienced by a probe droplet (accuracy $<\pm 0.2\%$ at 90% RH and above) and rapid retrieval of hygroscopic growth up to very high solution water activity (>0.995).The CK-EDB technique is used for accurate and reproducible measurement of the hygroscopicity of single, aqueous aerosol droplets composed of mixtures of organic compounds with systematically increasing complexity in chemical composition. The CK-EDB technique has significant advantages, including: rapid measurement time (< 20 s), precise determination of the RH within the trapping chamber, measurement of the equilibrium hygroscopic response of single aerosol particles at water activities close to saturation (>0.995) and unambiguous measurement of the solute effect without the need to correct for the Kelvin effect since the analysed droplets are in the micrometre size range. The validity of the CK-EDB technique in the determination of the hygroscopic response for both organic and inorganic solutes has been extensively evaluated in previous work.[31-33]

Here, we progressively increase the compositional complexity of the organic solute mixture to gain insight into the intermolecular interactions which govern the physical properties of the aerosol, further developing a method used by us in previous work.[34] We report measurements of the hygroscopic response of aerosol particles composed of the organic and amino acid mixtures shown in Table 1. Mixtures of these organic components were chosen for the following reasons. Firstly, the hygroscopicities of the binary aqueous mixtures

of the individual components in these mixtures have been measured in earlier work using the CK-EDB technique.[29] The availability of the binary aqueous-organic hygroscopic response for every component in each mixture allows an examination of the reliability of mixing rules for hygroscopicity (e.g. mixing rules for the κ parameter). Secondly, the presence of amino acids allows for an examination of non-additive behaviour due to the presence of charged chemical species, without the use of inorganic salts that can dominate the hygroscopic response when present in a mixture with other less hygroscopic organic species. In addition, the compounds chosen are sufficiently soluble to allow bulk phase measurements of refractive index and density, and cover a wide range of O:C ratios from 0.57 to 1.6. We now review the methods used before reporting measurements of refractive index, density and hygroscopicity.

## 2. Methods

A comparative kinetics technique is applied using an electrodynamic balance to retrieve the hygroscopic response of single aerosol particles, with the instrument henceforth referred to as the CK-EDB. The operation of the CK-EDB and the extraction of the hygroscopic response has been extensively discussed in previous publications [31-36] and as such will only be briefly discussed here. Initially droplets are ~25 μm in radius at the initial high water activity of the starting solution and evaporate to ~5 μm at the lowest water activity of the measured hygroscopic response. Working with such large droplets provides a direct approach for retrieving the thermodynamic response of the equilibrium solution composition to change in water activity/relative humidity, without a requirement to correct for the Kelvin effect and surface curvature.[31-33] A full schematic outlining the analysis procedure is shown in Scheme S1.

The CK-EDB utilises two droplet-on-demand generators to sequentially generate, probe and sample droplets. During generation, droplets are imparted charge by an induction electrode on droplet formation and confined within an electrodynamic field generated between a set of concentric cylindrical electrodes. The temperature of the trapping chamber is controlled by fluid from a refrigerated circulator; all measurements presented in this work are at 293 K. The relative humidity is modified by altering the relative ratio of a dry and wet nitrogen flow. Confined droplets are illuminated with a 532 nm laser and their size estimated using the geometrics optics approximation with an accuracy in radius of ±100 nm (eq. S1).[32, 37] The application of the geometric optics approximation relies on the knowledge of the refractive index of a droplet, which is calculated using the molar refraction mixing rule.[38, 39] The application of the molar refraction mixing rule for complex mixtures such as those considered in this work is discussed in section 3.1.

The gas phase RH, held steady over the course of a sequence of measurements, can be determined using a probe droplet of pure water at RHs > 80% (with accuracy higher than ±0.3%) or containing an aqueous solution of sodium chloride for RHs < 80% (with accuracy higher than ±1.2%).[31] A semi-analytical treatment, first introduced by Kulmala and co-workers [40] and described in the supplementary information (SI), is used to model the mass flux of water evaporating from the water probe droplet and used to determine the RH. In the case of

sodium chloride probe droplets, the growth factor at the equilibrated radius is used to determine the RH. The Kulmala mass flux equation is then applied to the sample droplet (i.e. the droplet containing the solute of unknown hygroscopicity) evaporating into a known gas phase RH in order to extract its hygroscopic response by inferring the water content at all of the intervening water activities the droplet must transition through when equilibrating to a steady composition at the gas phase RH. The range of applicability of the Kulmala kinetics model and the full retrieval of the equilibrium hygroscopic properties from multiple droplets is discussed by Rovelli et al.[27] The experimental approach has been benchmarked for a wide range of binary aqueous solution aerosol containing inorganic [31] and organic [33] solutes.

Hygroscopicity measurements are compared with predictions (in terms of mass fraction of solute, MFS) from the web version of the Aerosol Inorganic-Organic Mixtures Functional Groups Activity Coefficients model referred to throughout as AIOMFAC-web and available at http://www.aiomfac.caltech.edu/index.html.[41, 42] Additionally, measurements of the hygroscopicity parameter, κ, are compared with predictions from the University of Manchester System Properties (UManSysProp) model available at http://vm-woody009.itservices.manchester.ac.uk/.[43] Both AIOMFAC-web and UManSysProp utilise Universal Quasichemical Functional Group Activity Coefficients (or UNIFAC groups) to segment and represent organic molecules in terms of their functional groups.[44] The UNIFAC groups implemented for each mixture in this work are shown in the supplement (Table S4) and a full description of how molecules can be segmented into appropriate UNIFAC groups is available on the AIOMFAC-web help section.

## 3. Results and Discussion

### 3.1 Extension and Validation of the Molar Refraction Mixing Rule for Predicting the Refractive Index of Multi-Component Aqueous-Organic Mixtures

We first provide an assessment of the accuracy of molar refraction for predicting the RI and density of compositionally complex mixtures containing multiple solute components based on comparison with measurements of bulk solutions under sub-saturated conditions. The dependence of the solution refractive index on the solute concentration is required for the accurate determination of the size of droplets with the geometric optics approximation (see section S1) and, thus, for accurate retrieval of the hygroscopic response. In addition, a parameterisation of solution density is required for the application of the molar refraction mixing rule and the extraction of the hygroscopic response. More generally, the predictions of these properties must be robust in order to relate mass concentrations to size distributions of ambient aerosols and to calculate the radiative impacts of atmospheric aerosols.[45, 46] Thus, a rigorous assessment of estimation methods based on solutions of known properties is of considerable value.

The molar refraction mixing rule, normally implemented for single solute aqueous solutions[38] for the self-consistent treatment of both density and refractive index, is defined by eq. 1, where $R$ is molar refraction, $n$ is refractive index, $M$ is the molecular weight and $\rho_M$ is the mass density.

$$R = \left(\frac{n^2-1}{n^2+2}\right)\frac{M}{\rho_M} \quad (1)$$

In the work of Cai et al., bulk measurements of density and refractive index up to the solubility limit were taken for ~ 70 organic compounds in aqueous solutions.[39] These bulk data were used to parametrise density and refractive index across the entire mass fraction range (i.e. beyond the solubility limit). From Eq (1) the molar refraction mixing rule also requires parametrisation of solution density; Cai and co-workers determined that the best density parametrisation is dependent on the solubility of each compound. When the solute reaches its bulk solubility limit lower than a mass fraction of solute (MFS) of 0.4, ideal mixing is used to parametrise the solution density. When a solute has a bulk solubility MFS > 0.4, the density is best parametrised using a third order polynomial fit to $\rho_M$ vs √MFS.

Equations (2) to (4) can be used to estimate the molar refraction, density and molecular weight of the combined aqueous-organic solute mixture. The effective molar refraction $R_e$ of the solute mixture can be determined using eq. (2) using the sum of the molar refraction $R_i$ weighted by respective mole fractions $x_i$ of each solute component $i$.

$$R_e = \sum_i x_i R_i \quad (2)$$

The effective density, $\rho_{em}$, of the organic solute mixture can be predicted from the individual component densities using ideal mixing, defined in eq. (3), with the mass fraction of each solute, $\varphi_i$, and the pure component melt density of each solute, $\rho_i$.

$$\frac{1}{\rho_{em}} = \sum_i \frac{\varphi_i}{\rho_i} \quad (3)$$

The effective molecular weight, $M_e$, of the organic solute mixture can be determined using eq. (4) and it is defined as the sum of the mole fraction $x_i$ multiplied by the molecular weight $M_i$ for each solute component $i$.

$$M_e = \sum_i x_i M_i \quad (4)$$

Once values of $\rho_{em}$, $M_e$ and $R_e$ are obtained, the effective refractive index, $n_e$, of a mixture containing multiple components can be determined using eq. (5), which is a rearrangement of eq. (1) to solve for $n_e$.

$$n_e = \left(\frac{\left(2R_e+\left(\frac{M_e}{\rho_{em}}\right)\right)}{\left(\left(\frac{M_e}{\rho_{em}}\right)-R_e\right)}\right)^{1/2} \quad (5)$$

We report here bulk measurements of density and refractive index for the multicomponent mixtures listed in Table 1 up to the bulk solubility limit (tabulated values available in Table S1). We compare three methodologies in the application of the molar refraction mixing rule to parameterise solution refractive index.

1. From the data for the binary aqueous mixtures of organics collected by Cai *et al.*,[39] predictions of molar refraction, refractive index and density for aqueous organic mixtures with multiple solute components are performed using the sets of equations described above. These calculated properties from parameterisations of bulk phase data for binary solutions of each component in the mixture are referred to as binary-predicted values and notated as $\rho_{predicted}$ and $n_{predicted}$ :
   - $\rho_{predicted}$ – density of mixture determined using binary parametrisations from Cai *et al.*;
   - $n_{predicted}$ – refractive index of mixture determined by application of multicomponent molar refraction.

   Note this approach requires no bulk data of density and refractive index for the actual multicomponent mixtures studied here.

2. Bulk data of density and refractive index for the multicomponent mixtures studied here are used to parametrise across the entire mass fraction of solute (MFS) range for the specific fixed ratio of solutes. An ideal mixing treatment is used to parametrise the density of the aqueous solution. The fitting is performed using the same method as for binary solutions described by Cai *et al.*[39] The notation used is:
   - $\rho_{ideal}$ – ideal mixing treatment of bulk measurements of mixture density;
   - $n_{ideal}$ – refractive index determined using molar refraction where bulk measurements of mixture density have been treated using ideal mixing.

3. Bulk data of density and refractive index for the multicomponent mixtures studied here are used to generate a parametrisation across the entire mass fraction of solute (MFS) range. A polynomial fit is used to parametrise density. The fitting is performed using the same method as for binary solutions described by Cai *et al.*[39] The notation used is:
   - $\rho_{poly}$ – polynomial fitting to bulk measurements of mixture density;
   - $n_{poly}$ – refractive index determined using molar refraction where bulk measurements of mixture density have been treated using a polynomial fit.

RIs and densities estimated from the binary-predicted values or from fits to bulk measurements for mixture 5 are presented in Figure 1 as an example. The values of RI and density in the limit of pure solute (no water) are estimated using both methods 1 and 3, outlined above, with values for RI (1.464 and 1.463, respectively) and density (1.355 and 1.351 g $cm^{-3}$, respectively) in good agreement. For fits to aqueous solutions, these values provide estimates for the sub-cooled melts, rather than the crystalline phase, and can be considerably less than

the values for the corresponding pure solids.[39, 47, 48] A similar comparison is shown for mixture 7 in SI Figure S1, again with excellent agreement between the two methods across the entire MFS range.

As described earlier, the solubility of the solutes determines which density treatment is most appropriate to predict behaviour of the entire solution range. Mixture 7 is the least soluble mixture of all considered here and reaches its solubility limit at an MFS of just 0.0394. Thus, only an ideal mixing density treatment can be justified when fitting the bulk measurements of density. It is clear from Figure 1 and Table 1 that Mixture 5 is the most soluble of all the mixtures considered, and therefore a third order polynomial was used to parametrise its solution density across the entire MFS range. For Mixtures 1, 2, 4 and 6, the bulk solubility limits were very close to an MFS of 0.4, the threshold at which the appropriate density treatment is chosen. The impact of the density treatment applied to the measurements is examined for Mixture 1 in Figure 2 (a) – (b) with remaining Mixtures, 2, 4 and 6 presented in Figure S2. The parametrisations of mixture solution density are generated by applying either the ideal mixing density treatment (blue line) or the polynomial fit (black line) to the measured bulk solution values of density. Finally, three RI parametrisations are determined from the molar refraction mixing rule, considering the three density treatments: the binary-predicted $n_{predicted}$ (purple dashed line); the ideal fit to the bulk mixture experimental density data, $n_{ideal}$; and a polynomial fit to the bulk mixture experimental density data, $n_{poly}$. From Figure 2 it is evident that the chosen density treatment applied to the bulk measurements (3rd order polynomial or ideal mixing) gives pure solute (no water) melt densities and refractive indices that differ from the binary-predicted values for mixture 1 (and for mixtures 2, 4 and 6 shown in Figure S2). Therefore, it is important to establish to what extent the density treatment used influences the pure solute density and RI, their influence on the solution values, and their influence on the resulting hygroscopicity retrieved from the CK-EDB measurements for each of these mixtures.

The differences between the parametrisations informed by the bulk mixture measurements and the binary-predicted parametrisations are reported for the density and refractive index. First, the differences between the chosen density treatment applied to the bulk measurements (i.e. ideal mixing, $\rho_{ideal}$, or 3rd order polynomial fitting, $\rho_{poly}$) and the binary-predicted density ($\rho_{predicted}$) are examined. Overall, Figure 3 (a) and (b) show that the ideal mixing density treatment for the mixture data gives larger density and refractive index values than the binary-predicted values. In contrast, when a polynomial fit is used to parametrise the measurements (Figure 3 (c) and (d)), it is clear that the lower the solubility of the mixture, the larger the extrapolation in the polynomial fit and, therefore, the greater the disparity between $\rho_{poly}$ and $\rho_{predicted}$ and also refractive index at high MFS (e.g. mixture 3).

To establish how uncertainties in the density parametrisation influence the inferred hygroscopic behaviour from CK-EDB measurements, we have performed a sensitivity analysis on the retrieved hygroscopicity of Mixture 1, comparing the outcome using the different treatments for the refractive index and density. At lower RH, the error in density will have a more significant effect on the hygroscopic curve, reflecting the uncertainty of the pure component densities; on the other hand, at high water activities the density of water is well known

and, thus, the parametrisation is well constrained. The hygroscopicity data for mixture 1 was re-analysed using 4 density treatments (Table S1) corresponding to upper and lower error of ±2% and ±5% on the pure component density of 1.352 g·cm$^{-3}$ (determined using a binary-predicted parametrisation from values in in Cai et al.),[39] as shown in Figure 4. The shaded areas in Figure 4 represent the uncertainty in the retrieved hygroscopic response using the different density treatments. It is evident that both a ±2 and ±5% uncertainty in pure component density have minimal impact on the determined hygroscopic response. This conclusion agrees with a similar analysis that was conducted in a previous publication: Rovelli and co-workers demonstrated that a ±2% error in density did not impact significantly the estimated hygroscopicity for CK-EDB measurements of ammonium sulphate aerosol.[36]

In conclusion, Figure 4 demonstrates that bulk measurements of density and refractive index do not need to be performed for any further mixture combinations. In fact, parametrisations generated using information on the aqueous binary solutions of the individual compounds present in a mixture (binary-predicted) provide an adequate representation of the MFS dependence of density and refractive index, such that the hygroscopic measurement analysis is not compromised. The largest errors on the hygroscopicity retrieval have been discussed extensively in earlier work and are a result of the uncertainty in droplet sizing and on the thermophysical parameters implemented in the Kulmala equation, such as the gas phase diffusivity and thermal conductivity constants.[49] Thus, the binary-predicted parametrisations have been used in the analysis of the hygroscopic response; the pure component values and parametrisations used are listed in Table 2. Recognising that the comparison of the accuracies of the parameterisations can only be made up to the solubility limits of the bulk measurements, we adopt the same cautious approach as assessed in our previous study of binary solutions.[39] Using polynomial representations of the mixture density can lead to deviations and unphysical behaviour, particularly if the solubilities of the individual components are low. In our previous work,[39] optical tweezers measurements were used to assess the accuracy of different polynomial treatments of density to very low water activity/high solute saturation. For consistency with this, we base our treatments of the solution density and refractive index on the use of the molar refraction model and simple binary solution density data. However, we also recognise that the maximum deviation in solution density and RI for the mixtures studied here are typically no more than +/- 5% and +/- 5%, respectively.

### 3.2 The Hygroscopic Response of Aqueous-Organic Mixtures

The hygroscopic responses of all mixtures considered in this work are shown in Figure 5 (a) to (g). It is important to highlight that Mixtures 1 and 2 are characterised by similar O:C ratios, 0.8 and 0.77 respectively. This is relevant since the literature often reports correlations of O:C ratio with hygroscopicity or κ.[16, 17] Perhaps surprisingly, the overall hygroscopicity for both Mixtures 1 and 2 is dominated by the least hygroscopic component in their mixture (glutaric acid in both cases), with Mixture 2 apparently even less hygroscopic than glutaric acid (showing a higher mass fraction of solute, which means a lower water content, at the same water activity). This suggests that the hygroscopicity of a mixture is not simply additive. In addition, despite having

similar O:C ratios, Mixtures 1 and 2 have different hygroscopic properties providing an example of the inadequacy of simple correlations of the hygroscopic properties of organic aerosol particles and their O:C ratio.

In addition, at an RH lower than 80%, a kinetic limitation to water transport was observed for Mixture 2. The impact of high viscosity was evident in the processed hygroscopic curve; the viscosity, $\mu$, of this mixture of organic components is high enough at lower than 80 % RH ($\eta > 0.1$ Pa·s, the threshold established by Marsh et al.)[29] such that it influences the hygroscopicity measurement (shaded data points at RH < 80% reflect this). In addition to the non-additive hygroscopic behaviour observed for these mixtures, the increased viscosity of Mixture 2 also suggests that, whilst the binary aqueous-organic components do not have appreciable viscosity,[50] the viscosity of the mixture is not simply additive. As such the hygroscopicity of further mixture compositions were measured and are presented at ≥ 80% RH to ensure the measurements are not compromised by a kinetic limitation on water loss.

The hygroscopicity of Mixture 4 containing a mixture of amino acids (glycine and lysine) is shown in Figure 5 (d). Again, the hygroscopicity of Mixture 4 does not appear to behave additively, with its hygroscopicity tending to that of lysine, the least hygroscopic component of the mixture. This is an important observation which may aid the interpretation of the behaviour of five component mixtures with four organic solutes and water (i.e. Mixtures 1 and 2). The non-ideal interactions observed for Mixtures 1, 2 and 4 could originate from the presence of the amino acids which are zwitterionic, where the dicarboxylic acid is deprotonated, and this proton donated to the amine group. These charge interactions could play a role in non-additive hygroscopic behaviour of the more compositionally complex mixtures. It should be noted that lysine (146 g·mol$^{-1}$) is a much larger molecule than glycine (75 g·mol$^{-1}$) and this may explain why the hygroscopicity tends to that of lysine; this effect will be investigated in section 3.3. The amino acids present in the compositionally complex Mixtures 1 and 2, could be causing the non-additive hygroscopic behaviour observed. Mixture 1 is comprised of equimolar amounts of malonic and glutaric acids, glycine and lysine. To test the influence of amino acids on additivity, Mixture 6 should be considered. Although it is almost identical to Mixture 1, containing the same components, it contains double the molar amount of each of the amino acids, glycine and lysine, compared to malonic acid and glutaric acid. The hygroscopic response of Mixture 6 is shown in Figure 5 (f): it is evident that the hygroscopic response again tends to that of the least hygroscopic component (glutaric acid) even though the molar concentrations of amino acids, glycine and lysine (i.e. the most hygroscopic components), have been doubled. The doubling of the amino acid components and the resulting decrease in hygroscopicity further suggests that the presence of the zwitterionic amino acids is causing this non-additive hygroscopic behaviour. The hygroscopic response of Mixture 7 is presented in Figure 5 (g): clearly the hygroscopicity of the mixture is very similar to individual binary aqueous-organic constituents, which is unsurprising considering the similar hygroscopic response observed for its constituent components.

### 3.2.1 Potential Influence of Aerosol pH on Non-Additive Hygroscopic Behaviour

The hygroscopic behaviour of mixtures containing amino acids is non-additive as shown in Figure 5. One potential reason for this is that amino acids are zwitterionic and, in some cases here, also have additional proton accepting amine groups (specifically, lysine and arginine). The influence of this charge effect can be investigated by measuring the pH (HI 8314 Hanna Instruments) of the bulk aqueous mixture solution; measured pH values and the solution MFS are reported in Table 1. Of note are the acidic pH (0.61) of Mixture 3 containing oxalic and malonic acid and the alkaline pH (9.75) of Mixture 4 containing amino acids. As expected, it is clear from the measured pH values reported in Table 1 that, when amino acids are combined in aqueous solution with dicarboxylic acids, the pH of the resulting solutions (Mixtures 1, 2 and 6) are higher (i.e. more alkaline) than solutions containing dicarboxylic acids only. The amino acids act as proton acceptors and lead to an increase in pH. Indeed, lysine and arginine have one and three additional amine group(s), respectively. Importantly, aerosol droplets can become supersaturated with respect to solute concentration; thus, the pH of a droplet will differ from that of the starting bulk solution during evaporation (the values indicated in Table 1). Therefore, charge interactions and non-ideal behaviour would be exacerbated at low relative humidity and supersaturated solute concentrations in the droplet. For example, Rindelaub et al. measured the pH of droplets containing sulfuric acid impacted on a surface at humidities between 50-90% using Raman microscopy.[51] On drying (RH range 90 to 50%) droplets containing sulfuric acid (initial bulk solution pH 0.44-1.99) decreased in pH by 0.5 – 1. The evolving pH of an aqueous droplet containing glutaric acid can be estimated from the Extended-Aerosol Inorganics Model (E-AIM model III): between 90 and 40 RH%, the pH of the droplet increases from 2.05 to 3.3.[52] This stresses the importance of direct *in situ* measurements of aerosol particle pH with varying water activity, something that is not possible in these measurements and is only now becoming possible in other instruments.[51]

In the mixtures containing both acidic and basic components in supersaturated solution, charged species in solution could interact more strongly with their contact ion pairs than interactions via hydrogen bonding with water molecules, thereby supressing the hygroscopic response of the solute mixture.[53] In conclusion, available modelling methods and current experimental methods cannot be used to determine the pH at supersaturated solute conditions for mixtures of dicarboxylic and amino acids. Refined models that account for the changes in activity coefficient for these non-ideal solutions with variation in water activity are required. Moreover, measurement of the evolving pH of evaporating droplets containing the solute mixtures discussed was not possible in this work. However, the evidence presented above suggests that charge interactions play a role in the observed hygroscopicity, although we recognise the potential role of the zwitterionic form of the amino acids is speculative. Further work is required to fully elucidate the nuances of potential pH effects on the hygroscopic behaviour of the aerosol.

### 3.3 Comparison of the Measured Hygroscopic Response with Predicted Hygroscopic Behaviour

For each compound considered in this work, hygroscopic properties of the single component aqueous-organic solutions have been reported in Marsh et al.[29] This work presents a unique opportunity to test whether mixing rules can be applied to predict the hygroscopic response using, for example, the mass, mole and volume weighted kappa hygroscopicity parameter (κ) as defined in eq. (6)-(8). Here, $\varphi_i$, $x_i$ and $\varepsilon_i$ represent mass, mole and volume fraction respectively, and $\kappa_i(a_w)$ represents a water activity dependent kappa. The mass, $m_i$ and density, $\rho_i$ of the aqueous droplet can be used to determine the volume, $v_i$. The water activity dependent κ's for the binary aqueous-organic compounds, as determined by Marsh et al.,[29] were used with eq. (6)-(8) to predict the hygroscopic response of the mixtures studied in this work.

$$\kappa_{mass} = \sum_i \varphi_i \kappa_i(a_w) \quad (6)$$

$$\kappa_{mole} = \sum_i x_i \kappa_i(a_w) \quad (7)$$

$$\kappa_{vol} = \sum_i \varepsilon_i \kappa_i(a_w) = \sum_i \frac{m_i}{\rho_i} \kappa_i(a_w) \quad (8)$$

The experimentally measured hygroscopicity parameter κ is compared with predicted κ values determined using mass, mole and volume weightings and shown in Figure 6. The observed hygroscopic behaviour of Mixture 4 tends to that of the least hygroscopic component (lysine) consistent with Figure 5 (d). Glycine and lysine were combined in a 1 to 1 molar ratio; however, the molecular weight of lysine (146 $gmol^{-1}$) is almost double that of glycine (75 $gmol^{-1}$). Thus, in Figure 6 (d), the mass and volume weighted κ parametrisations are in better agreement with the experimental data than the mole weighted κ. However, the mass and volume weighted κ remain in poor agreement and this provides further evidence that the complex charge interactions between the zwitterionic amino acids could play a significant role in the observed hygroscopic behaviour.

Indeed, the influence of complex charge interactions between zwitterionic amino acids could also explain why the mass, mole and volume weighted predicted kappa values significantly disagree with experimental measurements for Mixtures 1, 2 and 6, presented in Figure 6 (a), (b) and (f) respectively. In Figure 5 (g), the predicted κ is clearly identical to the measured values, because all three components of the mixture are structural isomers of one-another and behave similarly. The predicted mass, mole and volume weighted values of κ, overestimate the experimentally determined κ values in every example considered here. It is evident from Figure 6 (a) to (f) that the predicted values of κ have minimal/limited overlap with the experimental CK-EDB measurements. These simple mixing rules for κ are not able to account for the solute concentration dependencies of the activity coefficients in the mixture and any synergistic interactions between different components in the mixture. As demonstrated in all examples in Figure 6, the results from the mixing rules highlight some significant discrepancies with the experimental data, especially in the low water activity range, even though they appear to somewhat capture the observed qualitative trends of complex mixtures. It should also be noted that the hygroscopicity "constant" κ varies by as much as a factor of 3 over the water activity range 0.8 to ~1.0 studied here. The potential interplay of the resulting uncertainties in representing the degree of hygroscopic growth, the RH dependence of the refractive index, and the impact on optical growth factor must be more fully explored to better quantify uncertainties in radiative forcing efficiency.[46]

In addition to examining the agreement of the mixing rules for κ, UManSysProp has been used to predict the hygroscopicity parameter κ as a function of water activity, shown in Figure 7(a).[43] For every mixture considered in this work, UManSysProp overpredicts the hygroscopic response (solid lines in Figure 6(a)). Figure 7(b) shows a correlation plot between either modelled κ from UManSysProp (solid symbols) or calculated κ using eq. (8) (open symbols) and the experimental measurement of the κ of each mixture (at $a_w$=0.95). UManSysProp over predicts κ when compared with the experimental value; this is consistent with what was observed in the work of Marsh et al., [29] where κ values for the binary aqueous-organic mixtures were similarly, but less significantly, overestimated by UManSysProp. Importantly, the hygroscopic parameters calculated from the binary component mixture data (open symbols) in Figure 7 are in significantly better agreement with the experimentally determined κ. This demonstrates the importance of experimental measurement of binary aqueous-organic hygroscopicity: not only can such measurements provide accurate treatments of complex solution mixture properties (density and refractive index), but they allow a better estimation of the calculated κ of the organic mixtures by using a volume weighted mixing rule.

AIOMFAC-web can also be used in the prediction of the hygroscopicity of mixtures; examples are shown in Figure 8 for Mixtures 3, 5 and 7. AIOMFAC-web was implemented for only these mixtures consistent with the applicability of the online version, i.e. AIOMFAC-web, which does not allow for the prediction of the amino acid species. AIOMFAC-web predictions for Mixtures 3 and 5 are in excellent agreement with experimental data. In contrast, experimental data for Mixture 7 is in less good agreement with the thermodynamic model prediction from AIOMFAC-web. In the work of Marsh et al.,[29] the hygroscopicity of the binary aqueous-organic mixtures for oxalic, malonic and glutaric acids were in excellent agreement with predictions from AIOMFAC-web, whereas all components from Mixture 7 were not in good agreement with AIOMFAC-web. This suggests that if the hygroscopicity of the individual compounds comprised within the mixture are well predicted by AIOMFAC-web, then the mixture itself is also well predicted and vice versa. However, we recognise that some additional measurement on mixtures of aqueous dicarboxylic acids would be needed to further confirm this conclusion.

## 4. Conclusions

In this work, experiments were performed using the CK-EDB technique to progressively examine the hygroscopic response of increasingly complex mixtures of organic compounds and to test the often used, but little validated, models for predicting mixture properties based on single component data and parameterisations. The focus of this work was therefore on complex mixtures of organic species, including linear and branched dicarboxylic acids and amino acids. First, the molar refraction mixing rule and the representation of mixture densities as a function of solute concentration were successfully extended to consider aqueous multi-component mixtures of organic solutes. Moreover, we demonstrated that bulk measurements of density and refractive index are not required for each mixture for an accurate determination of the hygroscopic

properties of aerosol particles with CK-EDB experiments (providing bulk data or equivalent parameterisations are available for the individual binary solutions). In fact, the molar refraction mixing rule using '*binary-predicted*' parametrisations of density and refractive index is sufficient so as not to compromise hygroscopicity determination (i.e. agreement with parametrisations generated using bulk data lies within ±2%). A caveat should be noted here that, whilst this level of accuracy is sufficient for the determination of hygroscopicity of single particles with our experimental approach, the determination of optical properties of aerosol particles with the aim for example of estimating their radiative forcing potential may require greater levels of accuracy under certain conditions. However, more work is required to evaluate use of molar refraction for these purposes. As an example, it was estimated that an uncertainty of 0.2% in refractive index for ammonium sulphate aerosol can results in a 1% error in calculated radiative forcing.[54] Therefore, further work is necessary to determine whether the molar refraction mixing rule is suitable for purposes other than the determination of the hygroscopic properties of single aerosol particles in CK-EDB experiments.

In Sections 3.2 and 3.3, measurements of hygroscopicity for 7 compositionally complex mixtures were performed using the CK-EDB. Mass, volume and mole weighted mixing rules for κ resulted in a moderate overprediction of κ for Mixtures 1 to 6. However, volume weighted calculated κ were significantly closer to experimental observations than predictions from UManSysProp. This demonstrates the importance of laboratory measurements on binary mixtures of organic solutes in order to be able to represent adequately the properties of more complex mixtures and, also, to provide data to inform the available prediction tools. Such an understanding is also crucial to understanding temporal trends in aerosol hygroscopicity when measured in the field and any attempt to rationalise these trends in terms of chemical composition.

The hygroscopicity of Mixtures 3 and 5 were well represented by their AIOMFAC-web predictions. The binary aqueous-organic hygroscopic properties of the constituent compounds of Mixture 3 and 5 (oxalic, malonic and glutaric acids) were well represented by AIOMFAC-web. In contrast, Mixture 7 was not well represented by the AIOMFAC-web model prediction, likely due to the poor prediction of the individual compounds present in Mixture 7 (pimelic, 2,2-dimethylglutaric and 3,3-dimethylglutaric acids). Generally, the mixtures represented well by thermodynamic model predictions were mixtures solely containing compounds whose binary aqueous-organic hygroscopic response (measured in Marsh et al.)[29] were well represented by thermodynamic model predictions (i.e. Mixtures 3 and 5).

Overall, this work has provided an assessment of the molar refraction mixing rule for multicomponent organic solute solutions, considered the efficacy of common mixing rules for κ and highlighted the non-additive hygroscopic behaviour of organic mixtures containing amino acids. Further research efforts are needed to better understand the non-ideality of complex mixtures and the impact of pH on their behaviour.

**Note**

The authors declare that they have no conflict of interest.

Data are available at the University of Bristol data repository, data.bris, at https://doi.org/10.5523/bris.3hfjvbpamxahs2p18s1qzligfv.

**Supporting Information**

The Supporting Information is available free of charge on the ACS Publications website at DOI:

Further discussion of the experimental procedure including droplet sizing procedure and extraction of hygroscopic response; additional figures and tabulated values of experimental data; and UNIFAC groups for thermodynamic predictions.

**Acknowledgments**

AM acknowledges the EPSRC for support through DTA funding. JPR and GR acknowledge NERC through funding from grant NE/N013700/1. REHM, AM and JPR acknowledge support from NERC through grant NE/N006801/1.

**References**

1. Ravishankara, A. R.; Rudich, Y.; Wuebbles, D. J. Physical Chemistry of Climate Metrics. *Chem. Rev.* **2015,** *115* (10), 3682-3703.

2. Moise, T.; Flores, J. M.; Rudich, Y. Optical Properties of Secondary Organic Aerosols and Their Changes by Chemical Processes. *Chem. Rev.* **2015,** *115* (10), 4400-4439.

3. Topping, D.; Connolly, P.; McFiggans, G. Cloud droplet number enhanced by co-condensation of organic vapours. *Nature Geosci.* **2013,** *6* (6), 443-446.

4. Haddrell, A. E.; Davies, J. F.; Reid, J. P. Dynamics of Particle Size on Inhalation of Environmental Aerosol and Impact on Deposition Fraction. *Environ. Sci. Technol.* **2015,** *49* (24), 14512-14521.

5. Hallquist, M.; Wenger, J. C.; Baltensperger, U.; Rudich, Y.; Simpson, D.; Claeys, M.; Dommen, J.; Donahue, N. M.; George, C.; Goldstein, A. H. et al. The formation, properties and impact of secondary organic aerosol: current and emerging issues. *Atmos. Chem. Phys.* **2009,** *9* (14), 5155-5236.

6. Pöschl, U.; Shiraiwa, M. Multiphase Chemistry at the Atmosphere–Biosphere Interface Influencing Climate and Public Health in the Anthropocene. *Chem. Rev.* **2015,** *115* (10), 4440-4475.

7. Ghio, A. J.; Carraway, M. S.; Madden, M. C. Composition of Air Pollution Particles and Oxidative Stress in Cells, Tissues, and Living Systems. *J. Toxicol. Env. Heal. B* **2012,** *15* (1), 1-21.

8. Reid, J. P.; Bertram, A. K.; Topping, D. O.; Laskin, A.; Martin, S. T.; Petters, M. D.; Pope, F. D.; Rovelli, G. The viscosity of atmospherically relevant organic particles. *Nat Commun.* **2018,** *9*.

9. Bzdek, B. R.; Power, R. M.; Simpson, S. H.; Reid, J. P.; Royall, C. P. Precise, contactless measurements of the surface tension of picolitre aerosol droplets. *Chem. Sci.* **2016,** *7* (1), 274-285.

10. Poschl, U.; Shiraiwa, M. Multiphase Chemistry at the Atmosphere-Biosphere Interface Influencing Climate and Public Health in the Anthropocene. *Chemical Reviews* **2015,** *115* (10), 4440-4475.

11. Kalberer, M.; Paulsen, D.; Sax, M.; Steinbacher, M.; Dommen, J.; Prevot, A. S. H.; Fisseha, R.; Weingartner, E.; Frankevich, V.; Zenobi, R.; Baltensperger, U. Identification of polymers as major components of atmospheric organic aerosols. *Science* **2004,** *303* (5664), 1659-1662.

12. Jimenez, J. L.; Canagaratna, M. R.; Donahue, N. M.; Prevot, A. S. H.; Zhang, Q.; Kroll, J. H.; DeCarlo, P. F.; Allan, J. D.; Coe, H.; Ng, N. L. et al. Evolution of Organic Aerosols in the Atmosphere. *Science* **2009,** *326* (5959), 1525-1529.

13. Bilde, M.; Barsanti, K.; Booth, M.; Cappa, C. D.; Donahue, N. M.; Emanuelsson, E. U.; McFiggans, G.; Krieger, U. K.; Marcolli, C.; Topping, D. et al. Saturation Vapor Pressures and Transition Enthalpies of Low-Volatility Organic Molecules of Atmospheric Relevance: From Dicarboxylic Acids to Complex Mixtures. *Chemical Reviews* **2015,** *115* (10), 4115-4156.

14. Yuan, C.; Ma, Y.; Diao, Y. W.; Yao, L.; Zhou, Y. Y.; Wang, X.; Zheng, J. CCN activity of secondary aerosols from terpene ozonolysis under atmospheric relevant conditions. *J Geophys Res-Atmos* **2017,** *122* (8), 4654-4669.

15. Petters, M. D.; Kreidenweis, S. M. A single parameter representation of hygroscopic growth and cloud condensation nucleus activity. *Atmos. Chem. Phys.* **2007,** *7*, 1961-1971.

16. Rickards, A. M. J.; Miles, R. E. H.; Davies, J. F.; Marshall, F. H.; Reid, J. P. Measurements of the Sensitivity of Aerosol Hygroscopicity and the κ. *J. Phys. Chem. A* **2013,** *117*, 14120−14131.

17. Duplissy, J.; DeCarlo, P. F.; Dommen, J.; Alfarra, M. R.; Metzger, A.; Barmpadimos, I.; Prevot, A. S. H.; Weingartner, E.; Tritscher, T.; Gysel, M.; Aiken, A. C.; Jimenez, J. L.; Canagaratna, M. R.; Worsnop, D. R.; Collins, D. R.; Tomlinson, J.; Baltensperger, U. Relating hygroscopicity and composition of organic aerosol particulate matter. *Atmos. Chem. Phys.* **2011,** *11* (3), 1155-1165.

18. Wang, Y. Y.; Jing, B.; Guo, Y. C.; Li, J. L.; Tong, S. R.; Zhang, Y. H.; Ge, M. F. Water uptake of multicomponent organic mixtures and their influence on hygroscopicity of inorganic salts. *J. Environ. Sci.* **2016,** *45*, 156-163.

19. Wu, Z. J.; Nowak, A.; Poulain, L.; Herrmann, H.; Wiedensohler, A. Hygroscopic behavior of atmospherically relevant water-soluble carboxylic salts and their influence on the water uptake of ammonium sulfate. *Atmos. Chem. Phys.* **2011,** *11* (24), 12617-12626.

20. Liu, Q. F.; Jing, B.; Peng, C.; Tong, S. R.; Wang, W. G.; Ge, M. F. Hygroscopicity of internally mixed multi-component aerosol particles of atmospheric relevance. *Atmos. Environ.* **2016,** *125*, 69-77.

21. Peng, C.; Jing, B.; Guo, Y. C.; Zhang, Y. H.; Ge, M. F. Hygroscopic Behavior of Multicomponent Aerosols Involving NaCl and Dicarboxylic Acids. *J. Phys. Chem. A* **2016,** *120* (7), 1029-1038.

22. Jing, B.; Tong, S. R.; Liu, Q. F.; Li, K.; Wang, W. G.; Zhang, Y. H.; Ge, M. F. Hygroscopic behavior of multicomponent organic aerosols and their internal mixtures with ammonium sulfate. *Atmos. Chem. Phys.* **2016,** *16* (6), 4101-4118.

23. Wang, X.; Jing, B.; Tan, F.; Ma, J.; Zhang, Y.; Ge, M. Hygroscopic behavior and chemical composition evolution of internally mixed aerosols composed of oxalic acid and ammonium sulfate. *Atmos. Chem. Phys.* **2017,** *17* (20), 12797-12812.

24. Mikhailov, E.; Vlasenko, S.; Rose, D.; Poschl, U. Mass-based hygroscopicity parameter interaction model and measurement of atmospheric aerosol water uptake. *Atmos. Chem. Phys.* **2013,** *13* (2), 717-740.

25. Marcolli, C.; Luo, B. P.; Peter, T. Mixing of the organic aerosol fractions: Liquids as the thermodynamically stable phases. *J. Phys. Chem. A* **2004,** *108* (12), 2216-2224.

26. Roberts, G. C.; Artaxo, P.; Zhou, J.; Swietlicki, E.; Andreae, M. O. Sensitivity of CCN spectra on chemical and physical properties of aerosol: A case study from the Amazon Basin. *J. Geophys. Res.-Atmos* **2002,** *107*, 8070.

27. Moore, R. H.; Raymond, T. M. HTDMA analysis of multicomponent dicarboxylic acid aerosols with comparison to UNIFAC and ZSR. *J. Geophys. Res.-Atmos* **2008,** *113*, D04206.

28. Lee, J. Y.; Hildemann, L. M. Comparisons between Hygroscopic Measurements and UNIFAC Model Predictions for Dicarboxylic Organic Aerosol Mixtures. *Advances in Meteorology* **2013,** *2013*, 897170.

29. Choi, M. Y.; Chan, C. K. The Effects of Organic Species on the Hygroscopic Behaviors of Inorganic Aerosols. *Environ. Sci. Technol.* **2002,** *36*, 2422-2428.

30. Suda, S. R.; Petters, M. D. Accurate Determination of Aerosol Activity Coefficients at Relative Humidities up to 99% Using the Hygroscopicity Tandem Differential Mobility Analyzer Technique. *Aerosol. Sci. Tech.* **2013,** *47* (9), 991-1000.

31. Rovelli, G.; Miles, R. E. H.; Reid, J. P.; Clegg, S. L. Accurate Measurements of Aerosol Hygroscopic Growth over a Wide Range in Relative Humidity. *J. Phys. Chem. A* **2016,** *120*, 4376−4388.

32. Davies, J. F.; Haddrell, A. E.; Rickards, A. M. J.; Reid, J. P. Simultaneous Analysis of the Equilibrium Hygroscopicity and Water Transport Kinetics of Liquid Aerosol. *Anal. Chem.* **2013,** *85* (12), 5819-5826.

33. Marsh, A.; Miles, R. E. H.; Rovelli, G.; Cowling, A. G.; Nandy, L.; Dutcher, C. S.; Reid, J. P., Influence of organic compound functionality on aerosol hygroscopicity: dicarboxylic acids, alkyl-substituents, sugars and amino acids. *Atmos. Chem. Phys.* **2017,** *17* (9), 5583-5599.

34. Marsh, A.; Rovelli, G.; Song, Y. C.; Pereira, K. L.; Willoughby, R. E.; Bzdek, B. R.; Hamilton, J. F.; Orr-Ewing, A. J.; Topping, D. O.; Reid, J. P. Accurate representations of the physicochemical properties of atmospheric aerosols: when are laboratory measurements of value? *Faraday Discuss* **2017,** *200*, 639-661.

35. Davies, J. F.; Haddrell, A. E.; Reid, J. P. Time-Resolved Measurements of the Evaporation of Volatile Components from Single Aerosol Droplets. *Aerosol. Sci. Tech.* **2012,** *46*, 666-677.

36. Rovelli, G.; Miles, R. E. H.; Reid, J. P.; Clegg, S. L. Hygroscopic properties of aminium sulfate aerosols. *Atmos. Chem. Phys.* **2017,** *17* (6), 4369-4385.

37. Glantschnig, W. J.; Chen, S.-H. Light scattering from water droplets in the geometrical optics approximation. *Appl. Opt.* **1981,** *20* (14), 2499-2509.

38. Liu, Y.; Daum, P. H. Relationship of refractive index to mass density and self-consistency of mixing rules for multicomponent mixtures like ambient aerosols. *J. Aerosol Sci.* **2008,** *39* (11), 974-986.

39. Cai, C.; Miles, R. E. H.; Cotterell, M. I.; Marsh, A.; Rovelli, G.; Rickards, A. M. J.; Zhang, Y.-H.; Reid, J. P. Comparison of Methods for Predicting the Compositional Dependence of the Density and Refractive Index of Organic–Aqueous Aerosols. *J. Phys. Chem. A* **2016,** *120* (33), 6604-6617.

40. Kulmala, M.; Vesala, T.; Wagner, P. An Analytical Expression For the Rate of Binary Condensational Particle Growth. *Proc. R. Soc. London. A* **1993,** *441*, 689-605.

41. Zuend, A.; Marcolli, C.; Luo, B. P.; Peter, T. A thermodynamic model of mixed organic-inorganic aerosols to predict activity coefficients. *Atmos. Chem. Phys.* **2008,** *8* (16), 4559-4593.

42. Zuend, A.; Marcolli, C.; Booth, A. M.; Lienhard, D. M.; Soonsin, V.; Krieger, U. K.; Topping, D. O.; McFiggans, G.; Peter, T.; Seinfeld, J. H. New and extended parameterization of the thermodynamic model AIOMFAC: calculation of activity coefficients for organic-inorganic mixtures containing carboxyl, hydroxyl, carbonyl, ether, ester, alkenyl, alkyl, and aromatic functional groups. *Atmos. Chem. Phys.* **2011,** *11* (17), 9155-9206.

43. Topping, D.; Barley, M.; Bane, M. K.; Higham, N.; Aumont, B.; Dingle, N.; McFiggans, G. UManSysProp v1.0: an online and open-source facility for molecular property prediction and atmospheric aerosol calculations. *Geosci. Model Dev.* **2016,** *9* (2), 899-914.

44. Fredenslund, A.; Jones, R. L.; Prausnitz, J. M. Group-contribution estimation of activity coefficients in nonideal liquid mixtures. *AIChE Journal* **1975,** *21* (6), 1086-1099.

45. Barley, M. H.; Topping, D. O.; McFiggans, G. Critical Assessment of Liquid Density Estimation Methods for Multifunctional Organic Compounds and Their Use in Atmospheric Science. *J Phys Chem A* **2013,** *117* (16), 3428-3441.

46. Valenzuela, A.; Reid, J. P.; Bzdek, B. R.; Orr-Ewing, A. J. Accuracy Required in Measurements of Refractive Index and Hygroscopic Response to Reduce Uncertainties in Estimates of Aerosol Radiative Forcing Efficiency. *J Geophys Res-Atmos* **2018,** *123* (12), https://doi.org/10.1029/2018JD028365.

47. Clegg, S. L.; Wexler, A. S. Densities and Apparent Molar Volumes of Atmospherically Important Electrolyte Solutions. 1. The Solutes H2SO4, HNO3, HCl, Na2SO4, NaNO3, NaCl, (NH4)2SO4,NH4NO3, and NH4Cl From 0 to 50 °C, Including Extrapolations to Very Low Temperature and to the Pure Liquid State, and NaHSO4, NaOH, and NH3 at 25 °C. *J. Phys. Chem. A* **2011,** *115*, 3393−3460.

48. Cai, C.; Marsh, A.; Zhang, Y.-H.; Reid, J. P. Group Contribution Approach to Predict the Refractive Index of Pure Organic Components in Ambient Organic Aerosol. *Environ. Sci. Technol.* **2017,** *51*, 9683−9690.

49. Miles, R. E. H.; Reid, J. P.; Riipinen, I. Comparison of Approaches for Measuring the Mass Accommodation Coefficient for the Condensation of Water and Sensitivities to Uncertainties in Thermophysical Properties. *J. Phys. Chem. A* **2012,** *116* (44), 10810-10825.

50. Song, Y. C.; Haddrell, A. E.; Bzdek, B. R.; Reid, J. P.; Bannan, T.; Topping, D. O.; Percival, C.; Cai, C. Measurements and Predictions of Binary Component Aerosol Particle Viscosity. *J. Phys. Chem. A* **2016,** *120* (41), 8123-8137.

51. Rindelaub, J. D.; Craig, R. L.; Nandy, L.; Bondy, A. L.; Dutcher, C. S.; Shepson, P. B.; Ault, A. P. Direct Measurement of pH in Individual Particles via Raman Microspectroscopy and Variation in Acidity with Relative Humidity. *J. Phys. Chem. A* **2016,** *120* (6), 911-917.

52. Clegg, S. L.; Brimblecombe, P.; Wexler, A. S. Thermodynamic model of the system $H^+$-$NH_4^+$-$Na^+$-$SO_4^{2-}$-$NO_3^-$-$Cl^-$-$H_2O$ at 298.15 K. *J. Phys. Chem. A* **1998,** *102* (12), 2155-2171.

53. Guo, X.; Shou, J. J.; Zhang, Y. H.; Reid, J. P. Micro-Raman analysis of association equilibria in supersaturated NaClO4 droplets. *Analyst* **2010,** *135* (3), 495-502.

54. Zarzana, K. J.; Cappa, C. D.; Tolbert, M. A. Sensitivity of Aerosol Refractive Index Retrievals Using Optical Spectroscopy. *Aerosol. Sci. Tech.* **2014,** *48* (11), 1133-1144.

55. Aristov, I. V.; Bobreshova, O. V.; Strel'nikova, O. Y. Glycine and L-lysine ionization in a mixed aqueous solution. *Russ. J. Electrochem.*+ **2002,** *38* (5), 567-569.

**TABLES**

**Table 1: S**ummary of the compounds in each mixture with the number of moles of that solute in brackets. An approximate solubility limit for each mixture is also reported, which is the maximum MFS at which solutes dissolved. The O:C ratio of each mixture and the solution mixture pH at the stated MFS are also reported.

| #Mixture | Mixture 1 | Mixture 2 | Mixture 3 | Mixture 4 | Mixture 5 | Mixture 6 | Mixture 7 |
|---|---|---|---|---|---|---|---|
| **Component 1** | Glycine (1) | Methyl Succinic Acid (1) | Oxalic Acid (1) | Glycine (1) | Glutaric Acid (1) | Glycine (2) | 3,3-Dimethyl Glutaric Acid (1) |
| **Component 2** | Lysine (1) | Arginine (1) | Malonic Acid (1) | Lysine (1) | Malonic Acid (1) | Lysine (2) | 2,2-Dimethyl Glutaric Acid (1) |
| **Component 3** | Glutaric Acid (1) | Glutaric Acid (1) | | | | Glutaric Acid (1) | Pimelic Acid (1) |
| **Component 4** | Malonic Acid (1) | Citric Acid (1) | | | | Malonic Acid (1) | |
| **Solubility Limit** | 0.3858 | 0.3260 | 0.1657 | 0.3717 | 0.5288 | 0.3610 | 0.0394 |
| **O:C Ratio** | 0.8 | 0.77 | 1.6 | 0.571 | 1 | 0.8 | 0.571 |
| **Measured pH of Bulk Solution (MFS)** | 3.44 (0.13) | 3.16 (0.08) | 0.61 (0.08) | 9.75 (0.08) | 1.38 (0.08) | 4.49 (0.16) | 2.35 (0.03) |
| **Literature value of pH** | | | | 9.52 [55] | | | |

**Table 2:** Refractive index and density parametrisations, used in the analysis of mixtures presented in this work ($\rho_{sol}$ is the density of the solution in $kg \cdot m^{-3}$ with $\varphi$ representing the MFS).

| Mixture | RI | Density / $gcm^{-3}$ | $\rho_{sol} = a + b\varphi^{1/2} + c\varphi + d\varphi^{3/2}$ | | | |
|---|---|---|---|---|---|---|
| | | | a | b | c | d |
| Mixture 1 | 1.5200 | 1.3526 | 998.2 | 43.803 | 67.102 | 241.45 |
| Mixture 2 | 1.52638 | 1.38503 | 997.94 | 47.53 | 68.84 | 269.91 |
| Mixture 3 | 1.48356 | 1.56608 | 997.95 | 158.03 | -249 | 655.82 |
| Mixture 4 | 1.58407 | 1.35483 | 997.4 | -26.81 | 457.33 | -186.58 |
| Mixture 5 | 1.46387 | 1.35079 | 997.4 | 7.76 | 250.84 | 99.36 |
| Mixture 6 | 1.54016 | 1.35549 | 997.4 | -27.04 | 439.76 | -61.65 |
| Mixture 7 | 1.48947 | 1.22248 | 998.05 | 16.72 | 108.14 | 99.02 |

**FIGURES**

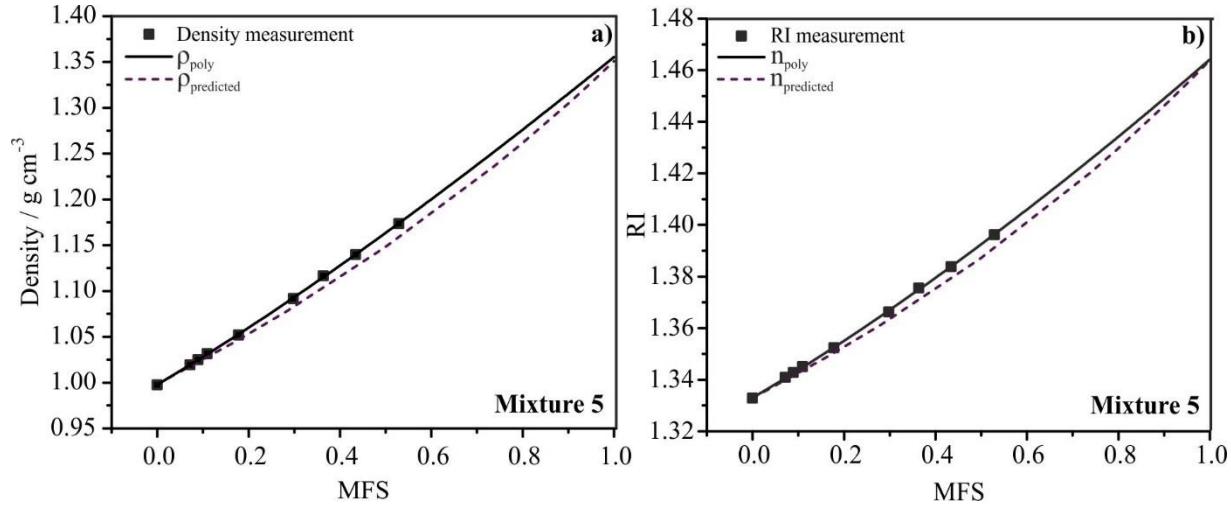


**Figure 1:** Mixture 5 (a) density and (b) RI as a function of MFS. In both (a) and (b), bulk measurements of aqueous mixture density and refractive index are shown (black solid squares) alongside the parametrisation of measurements (black solid line). The binary-predicted values are also shown (purple dashed line).

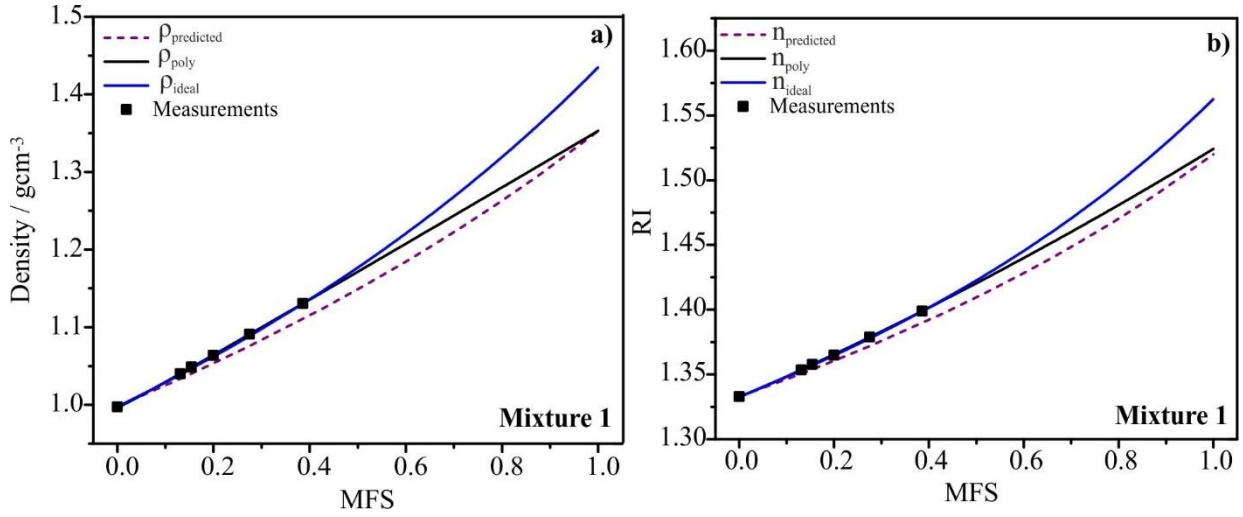


**Figure 2:** Mixture 1 (a) density and (b) RI as a function of MFS. In both (a) and (b), bulk measurements of aqueous mixture density and refractive index are shown (black solid squares) alongside the parametrisation of measurements using the two possible density treatments i.e. polynomial fitting (black line) and ideal mixing (blue line). The binary-predicted values are also shown (purple dashed line).

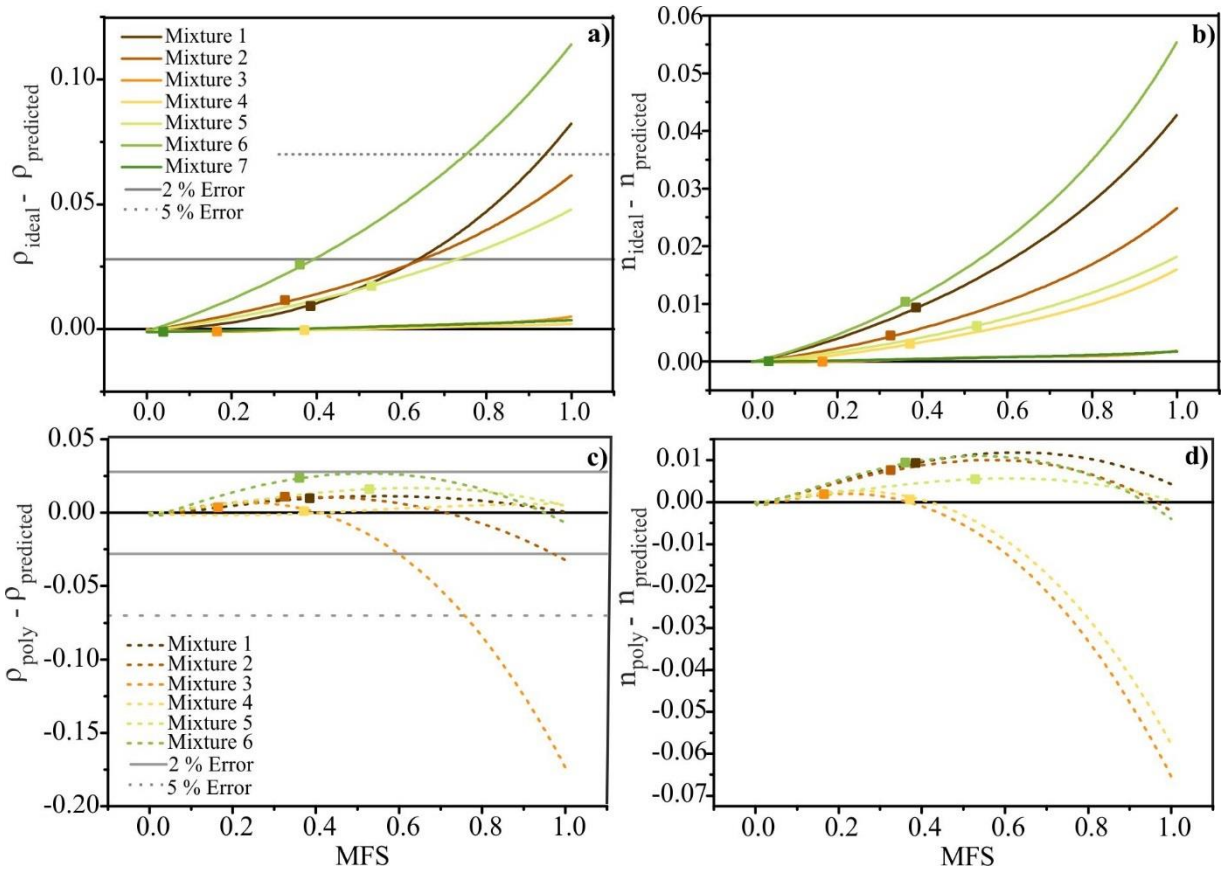


**Figure 3:** In (a) and (b) $\rho_{ideal}$ - $\rho_{predicted}$ values against MFS (solid lines) for all mixtures. In (c) and (d) $\rho_{poly}$ - $\rho_{predicted}$ values against MFS (dashed lines) for all mixtures. In (a) - (d) solid squares indicate the maximum solubility of bulk measurement taken for each mixture.

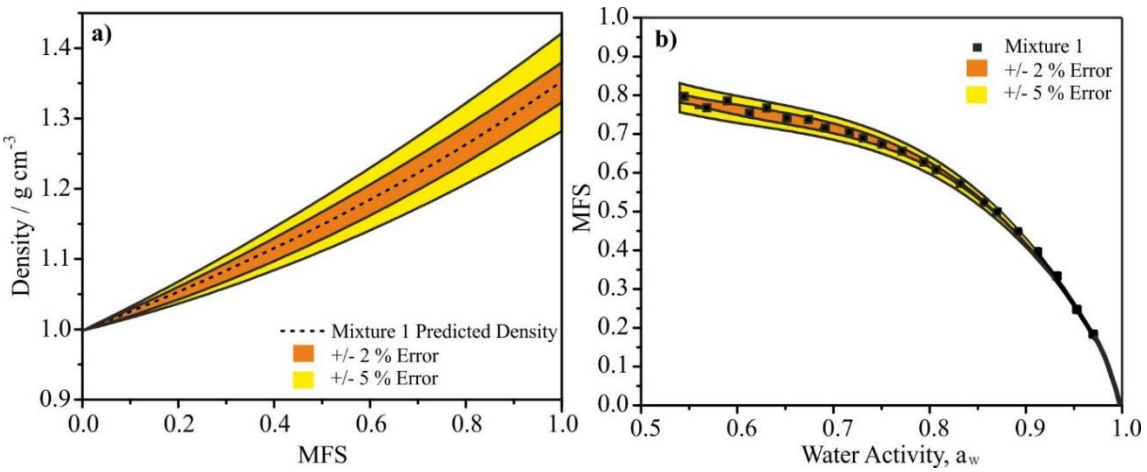


**Figure 4:** In (a) density vs. MFS and (b) MFS vs. water activity for Mixture 1 (glycine, lysine, glutaric and malonic acids). Orange and yellow shaded areas correspond to a ± 2 and ± 5% errors in pure component density, respectively.

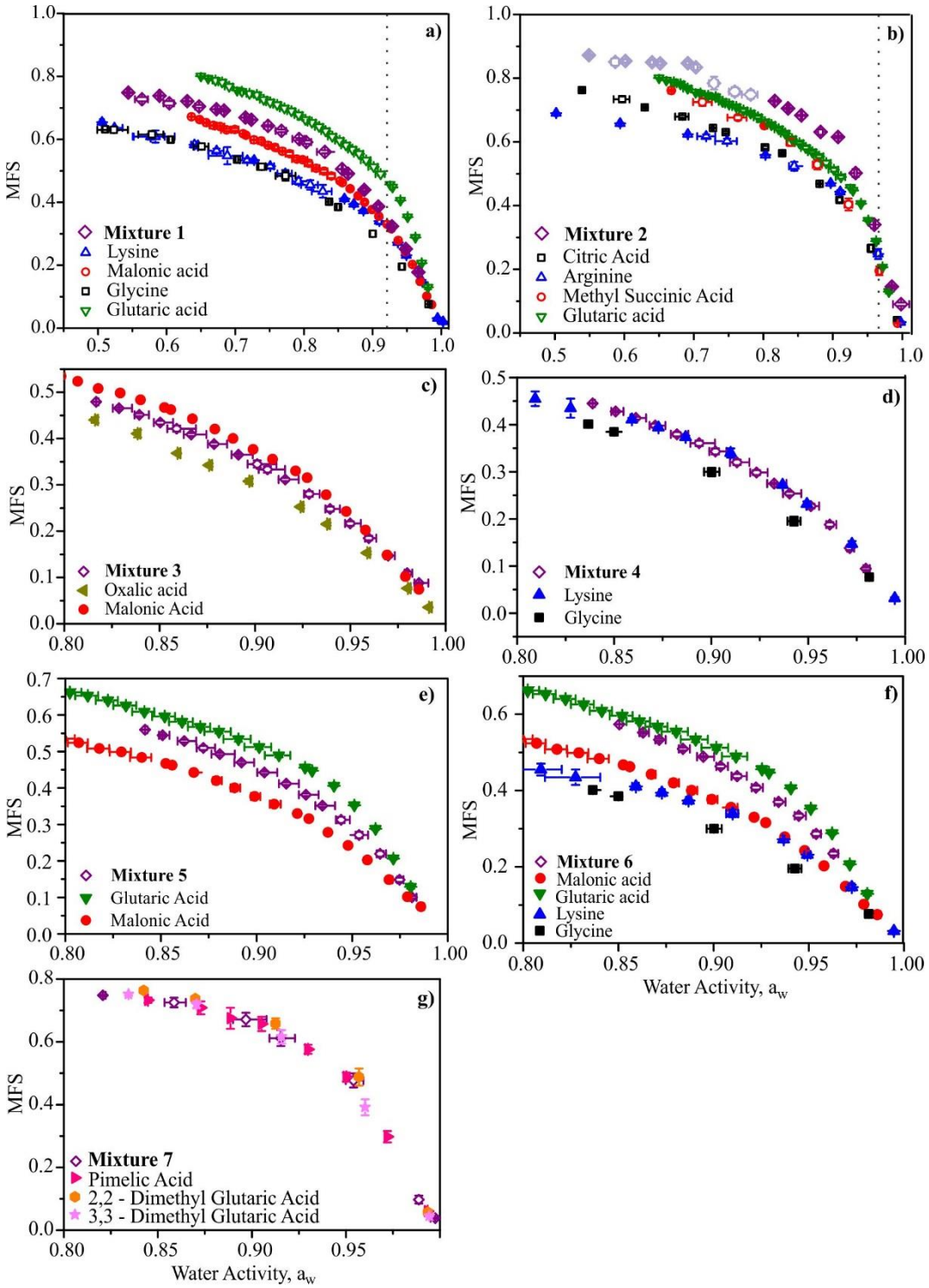


**Figure 5:** In (a)-(g) hygroscopicity represented in terms of MFS vs. water activity for Mixtures 1 - 7.

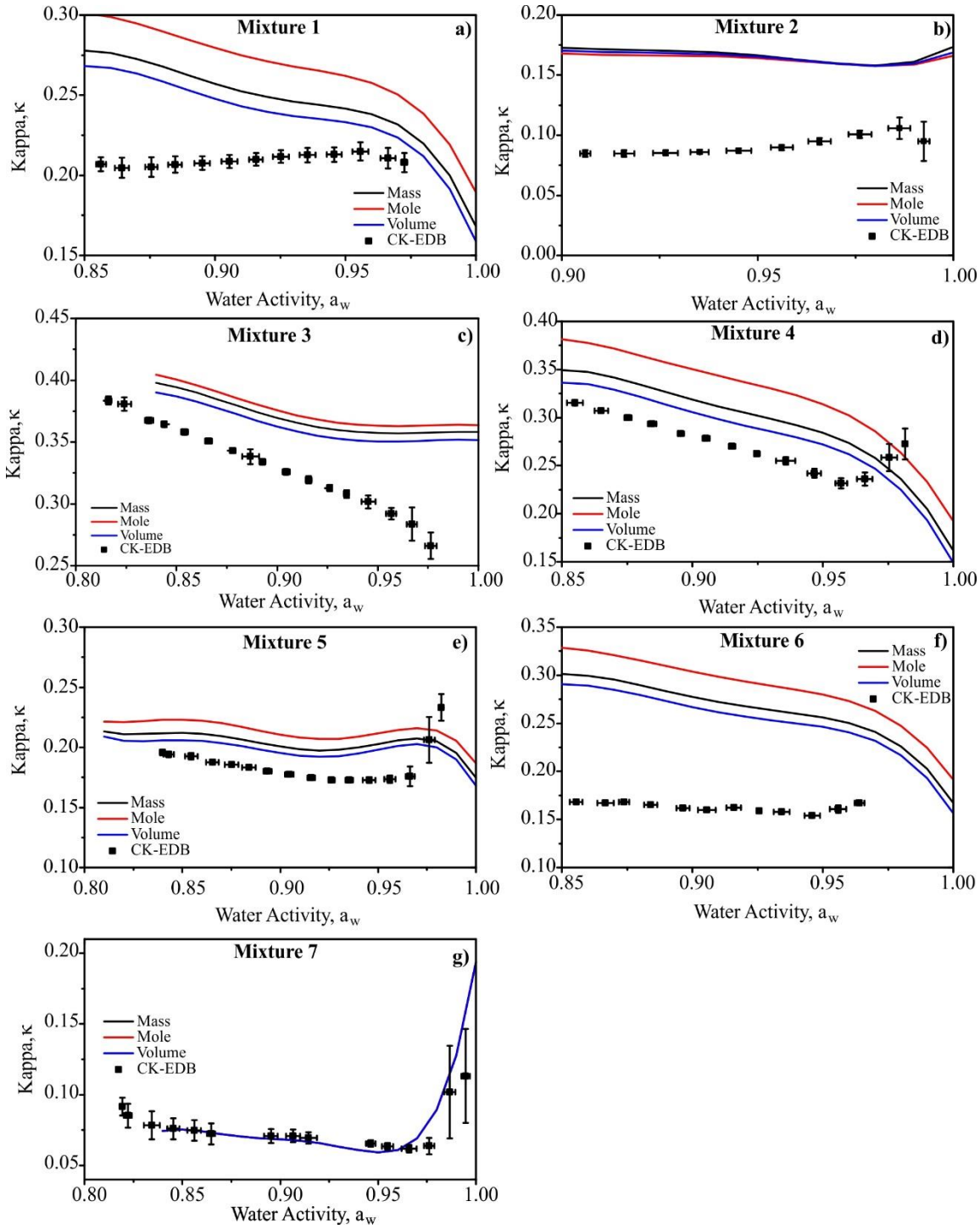


**Figure 6:** In (a) to (g), κ vs. water activity for all Mixtures 1-7. CK-EDB measurements (solid black squares) Are reported together with predicted κ using eq. 6, 7 and 8 for mass (black solid line), mole (red solid line) and volume (blue solid line) weighted individual components κ.

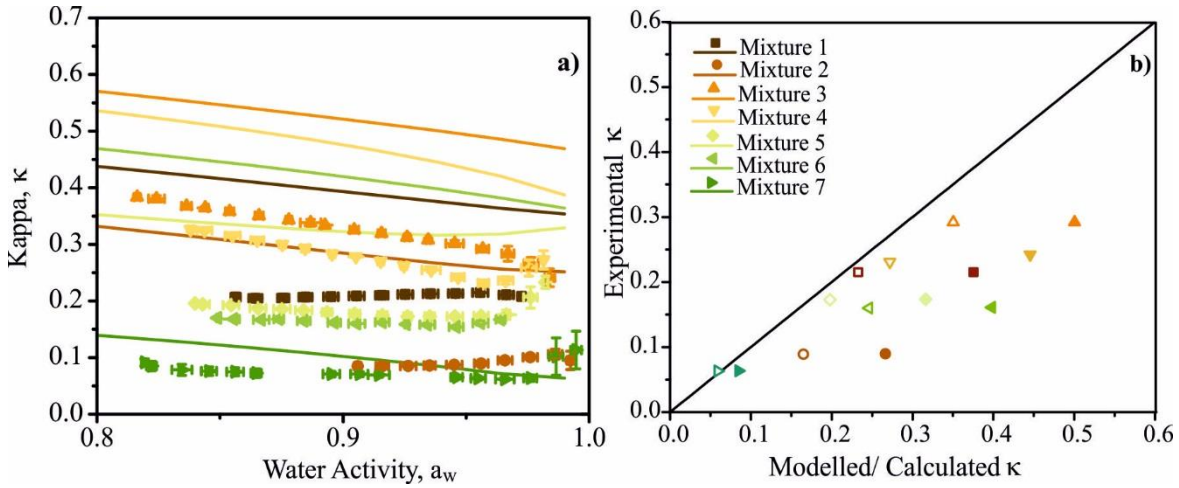


**Figure 7:** Hygroscopicity parameter κ against water activity for all mixtures. (a) CK-EDB measurements (data points) and UManSysProp thermodynamic predictions (solid lines). (b) Correlation plot of modelled κ, from UManSysProp (solid points) or volume weighted κ calculated from binary measurements (open symbols) both against measured experimental κ at $a_w$ = 0.95. Key for (a) and (b) provided in (b).

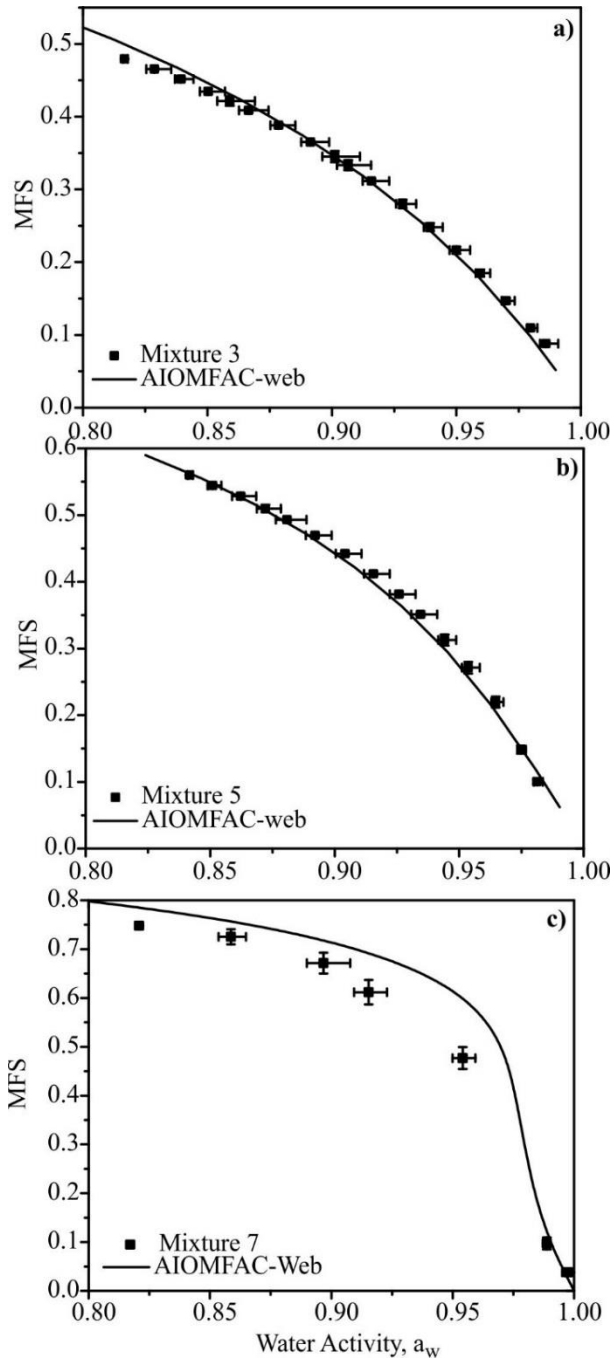


**Figure 8:** MFS vs. water activity CK-EDB measurements (black squares) for Mixture 3 (oxalic and malonic acid) in (a), Mixture 5 (glutaric and malonic acid) in (b) and Mixture 7 (pimelic, 2,2-dimethylglutaric and 3,3-dimethylglutaric acids) in (c). In all panels AIOMFAC-web predictions are shown (solid black line). UNIFAC functional groups used to represent each mixture are listed in supplement Table S4.

**TOC Graphic**